A new image reconstruction method to improve noise properties in x-ray differential phase contrast computed tomography

Ke Li[a], Nicholas Bevins[a], Joseph Zambelli[a], Guang-Hong Chen[a,b]

[a]Department of Medical Physics, University of Wisconsin-Madison, WI 53705;
[b]Department of Radiology, University of Wisconsin-Madison, WI 53792;

ABSTRACT

The noise properties of differential phase contrast CT (DPC-CT) demonstrate some peculiar features. It has been both theoretically and experimentally demonstrated that the noise variance of DPC-CT scales with spatial resolution following an inverse first order relationship. This is in stark contrast to absorption CT, where the noise variance scales with spatial resolution following an inverse third power. In addition to the scaling relationship, the noise power spectrum (NPS) of DPC-CT is dominated by low spatial frequencies and demonstrates a singular behavior when approaching zero frequency. This focuses the peak noise power within low spatial frequencies while high-frequency noise is suppressed. This is again in contrast to the absorption CT case where the NPS smoothly transitions to zero at zero frequency. The singular behavior of the DPC-CT NPS visually affects image noise texture and may hinder observer perception. In this paper, a method is proposed to improve the noise properties in DPC-CT and potentially improve observer performance. Specifically, the low frequency component of the filtering kernel used in reconstruction has been regularized to modify the noise power at low spatial frequencies. This results in a high-pass filtering of the image. The high-pass filtered image is combined with the original image to generate the final image. As a result of these two operations, the noise power is shifted to the high spatial frequency direction, improving visual perception, while image reconstruction accuracy is maintained. Experimental phantom results are presented to validate the proposed method.

Keywords: CT, x-ray phase contrast, detectability index, noise texture

1. INTRODUCTION

Recently, a breakthrough has been made in the x-ray physics community. Using a grating-based setup,[1–3] the measurement of refraction angle has been turned into a measurement of a phase offset of intensity modulations at the plane of the x-ray detector. Similar to absorption CT, when the refraction angles are properly measured from many view angles around the image object, one can reconstruct the distribution of the decrement from the index of refraction δ and display it as a differential phase contrast CT (DPC-CT) image.[4–6] The true benefits of the phase sensitive imaging method should be evaluated along with its noise properties. Recently, it has been experimentally demonstrated that the contrast to noise ratio (CNR) of DPC-CT can be higher than the CNR of absorption CT at the equivalent radiation dose level and spatial resolution level.[6] Further potential benefits of DPC-CT are suggested by a peculiar scaling law of noise variance vs spatial resolution.[7] For a two-dimensional image slice, it has been theoretically and experimentally demonstrated that the noise variance in DPC-CT scales with spatial resolution following an inverse power law with an exponent of one, while the noise variance in absorption CT scales with spatial resolution following an inverse power law with exponent three. Thus, for high spatial resolution imaging, DPC-CT has potential benefits.

However, the potential benefits of DPC-CT also come with some potential caveats for practical applications. In both numerical simulations[8,9] and experimental studies,[10] a peculiar noise power spectrum (NPS) has been observed: the NPS diverges as it approaches zero spatial frequency, but singularly drops back to zero at zero spatial frequency. This leads to a dramatic shift of the noise power to the low spatial frequency region and makes the visual appearance of DPC-CT images far different from that of absorption CT images. This peculiarity in the NPS may also have an important impact on human observer performance in practice and deserves a thorough study. Therefore, it is highly desirable to develop a systematic method to tailor the noise behavior of DPC-CT

Medical Imaging 2012: Physics of Medical Imaging, edited by Norbert J. Pelc, Robert M. Nishikawa, Bruce R. Whiting,
Proc. of SPIE Vol. 8313, 83131V · © 2012 SPIE · CCC code: 1605-7422/12/$18 · doi: 10.1117/12.911604

such that the potential benefits can be maintained while the potential detrimental effects of the peculiar NPS can be mitigated for a practical application.

A natural choice to address this peculiar NPS issue is to use filters that suppress the low frequency noise. In a simulation study, Raupach and Flohr[9] used a high-pass filter in the filtered backprojection (FBP) reconstruction of DPC-CT images. The resulting images have a noise texture similar to that of the FBP-reconstructed absorption CT images. However, since this method abandons the use of the well-established Hilbert-filter-based FBP reconstruction of DPC-CT, the resulting images are no longer quantitatively proportional to the decrement δ. The images have enhanced edges but decreased contrast between a homogeneous object and the surrounding air.

In this paper, we present a new approach to improve the noise texture of DPC-CT images while maintaining the reconstruction accuracy of the final DPC-CT images. A favorable noise texture and better object perceptibility can be realized in DPC-CT using this method. Instead of directly using a high-pass filter to suppress low spatial frequency noise, we trace the singularity in the NPS back to the singularity in the Hilbert kernel used in image reconstruction. It is the discontinuity of the Hilbert kernel at zero spatial frequency that causes the singular behavior of the NPS. Thus, proper regularization of the Hilbert kernel at zero frequency can control the amount of frequency shift in NPS. however, the reconstruction accuracy is degraded with the regularization of the filtering kernel. A weighted combination scheme is thus proposed to combine the non-regularized and regularized reconstruction to balance the noise properties and reconstruction accuracy. Experimental studies have been performed to validate the proposed method.

2. METHODS AND MATERIALS

2.1. Reweighted DPC-CT Reconstruction

Filtering DPC projection data with a Hilbert kernel before backprojection has become the standard for the reconstruction of DPC-CT images.[11] The Hilbert kernel is expressed as

$$H(k) = -i\pi \mathrm{sgn}(k), \tag{1}$$

where k denotes spatial frequency. During the FBP reconstruction of a DPC-CT image, the backprojection process more densely fills the low frequency portion of the 2D Fourier transform of the image. A problem with the Hilbert kernel is that it puts equal weight over all points of the projection data (ignoring the sign of the weight) in k-space, thus not helping to improve the ultra-unbalanced frequency distribution. A second problem with the Hilbert kernel is that it is discontinuous about $k = 0$.

In this paper, a hyperbolic tangent (tanh) function kernel is proposed as the high pass filter in the image reconstruction of DPC-CT. The tanh filter is defined as

$$T(k) = -i\pi \tanh\left(\frac{k}{k_0}\right), \tag{2}$$

where the tanh is given by

$$\tanh(k) = \frac{e^{k/k_0} - e^{-k/k_0}}{e^{k/k_0} + e^{-k/k_0}}. \tag{3}$$

Parameter k_0 has the same units as k and is used to shrink ($0 < k_0 < 1$) or dilate ($k_0 > 1$) the tanh filter along the k axis as shown in Figure 1. By varying k_0, the tanh function is equivalent to a high-pass filter with a tunable cut-off frequency. In the limit of $k_0 = 0$, $\tanh(k/k_0)$ is similar to sgn(k) except at $k = 0$, where the tanh function is continuous while the sgn function is discontinuous. Therefore, the tanh filter is selected as a substitute for the Hilbert filter to boost the high frequency content of the DPC-CT image.

Image distortion has been reported with the use of a high-pass filter in DPC-CT[9] reconstruction. Therefore, a reweighting method is proposed here to maintain reconstruction accuracy while improving the noise properties of DPC-CT. As shown in Figure 2, the proposed reweighted reconstructed DPC-CT image is a weighted sum of two images. The first image $\mathbf{X}_{Hilbert}$ is a standard DPC-CT image reconstructed using the well-established Hilbert kernel. Ignoring fluctuations caused by noisy projection data, its pixel value accurately represents the

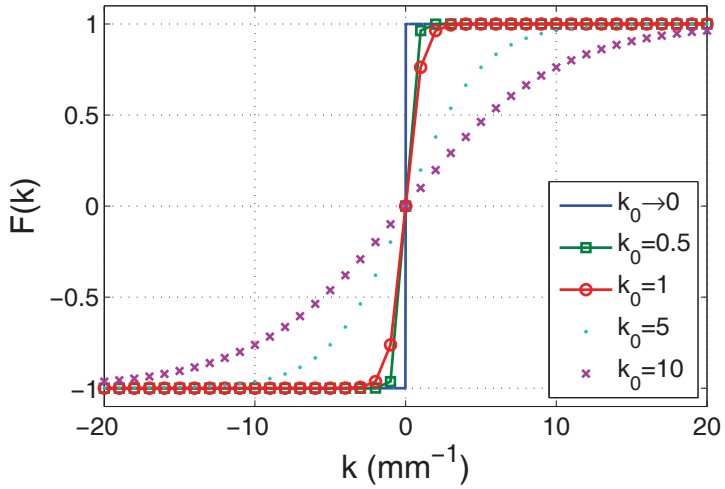

Figure 1. Hyperbolic tangent (tanh) functions in the spatial frequency (k) domain. The curves are similar in shape to typical high pass filters, with the threshold frequency controlled by parameter k_0. When $k_0 \to 0$, tanh becomes the sgn function (Hilbert filter). The k_0 and k parameters in the plot have the same units.

distribution of δ. The second image $\mathbf{X}_{\tanh}$ is reconstructed using the tanh kernel. The parameter α is used to put different weights on the two images before summation. This reweighted reconstruction algorithm is summarized in Equation 4,

$$\mathbf{X}_w = (1-\alpha)\mathbf{X}_{Hilbert} + \alpha\mathbf{X}_{\tanh}. \tag{4}$$

2.2. Validation of the Method

The proposed method was evaluated using experimental phantom data. The DPC data acquisition was done using a grating-based benchtop DPC-CT system constructed at UW-Madison. A standard rotating-anode diagnostic x-ray tube (Varian G1582, Palo Alto, CA) was used as the x-ray source. A CMOS detector (Rad-icon Shad-o-Box 2048, Sunnyvale, CA) was used with raw projection images 2×2 binned, which gives a 96×96 μm^2 pixel size. The physical phantom is a water cylinder with 4 cylindrical inserts, composed of PMMA, PTFE, POM, and air. The phantom has an outer diameter of 28.3 mm and wall thickness of 1.5 mm. An illustration of the phantom is shown in Figure 3. The phase contrast properties of all the materials used in this phantom have been previously reported.[6] For the CT acquisition, 360 projections was taken with a 1° angular interval, with the x-ray tube operated at 40 kVp and 20 mA. Each projection had an exposure time of 40 seconds, divided over the 8 phase steps. To measure the noise properties, two DPC-CT scans were acquired to generate two datasets

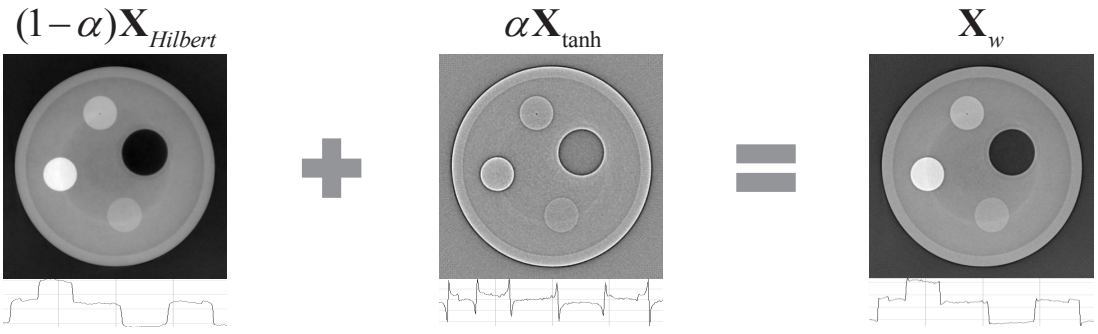

Figure 2. Illustration of the reweighted DPC reconstruction algorithm. Sample line profiles under each CT image demonstrate different edge and noise characteristics.

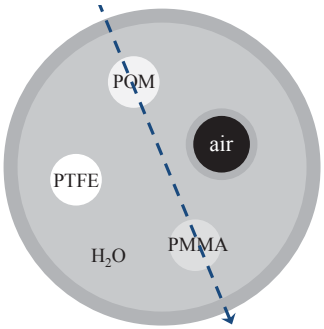

Figure 3. Schematic of the physical phantom used in the study. The outer diameter of the phantom is 28 mm. The dashed line marks the line profile shown in Figure 5a.

for the purpose of image subtraction. The reconstructed DPC-CT matrix size is 400×400 with a pixel size of 80×80 μm^2.

2.3. Evaluation Metrics

Along with line profiles of the images, NPS and point spread function (PSF) metrics were used to evaluate the proposed method.

2.3.1. Noise power spectrum (NPS)

Two-dimensional (2D) noise power spectra were calculated using the relation[12]

$$\mathrm{NPS}(u,v) = \frac{1}{N}\sum_{i=1}^{N} \frac{\left|DFT_{2\mathrm{D}}\left[\Delta I_i(x,y) - \overline{\Delta I_i}\right]\right|^2}{2} \frac{\Delta x}{N_x}\frac{\Delta y}{N_y}, \tag{5}$$

where N is the total number of sampled ROIs, N_x and N_y are the number of elements along each direction of the ROI, Δx and Δy are the corresponding physical pixel dimensions along each direction, and ΔI_i denotes the noise-only ROI of index value i. In this experiment, $\Delta x = \Delta y = 0.080$ mm, $N_x = N_y = 350$ for an ROI centered within the water cylinder, and $N = 100$ (100 CT slices). Due to the radial symmetry of the 2D NPS of DPC-CT,[10] a 1D NPS was calculated by radial averaging of the 2D NPS.

2.3.2. Pseudo point spread function (pseudo-PSF)

With a known ground truth, the sharpness of the reconstructed phase image can be quantified using the pseudo point spread function (pseudo-PSF).[13] The blur of an object (the PTFE rod) was modeled as a convolution with a Gaussian kernel. Given a 1D segment $\vec{x}$ through the object of interest in the reconstructed image, the shape of the kernel is given by solving the least squares problem

$$\min_{w,h} \left\| \vec{x} - hG_{w,s} * \vec{x}^{\mathrm{ref}} \right\|_{\ell_2}^2, \tag{6}$$

where h is a multiplicative factor, $\vec{x}^{\mathrm{ref}}$ is the known object profile, and G_w is a Gaussian function

$$G_{w,s}(x) = \exp\left[-\frac{d^2}{2w^2}\right]. \tag{7}$$

The value of w and d that solve the least squares problem in Equation 6 are used as a metric of image sharpness.

3. RESULTS

Compared with the DPC-CT image reconstructed using the standard Hilbert filter, the reweighted DPC-CT images demonstrate improved edge definition (Figure 4). The overall texture of the reweighted images is also changed, as observed in the noise-only images in the bottom row of Figure 4. DPC-CT images reconstructed using a Hilbert filter alone ($\alpha = 0$) are dominated by highly-correlated low-frequency noise, and thus lack visual acuity. By increasing the weighting of the high-pass filtered image (i.e., increasing α) the level of "graininess" in the final image increases.

All the DPC-CT images in the top row of Figure 4 are displayed using the same window ([-δ_{H_2O}, 3δ_{H_2O}]), indicating that the method did not distort the image in the uniform region (low frequency information). This is highlighted by the line profiles in Figure 5, where the smooth features of the water cylinder and the rods were preserved in the reweighted images while all of the edges were enhanced.

The difference in the noise texture between the images in Figure 4 was quantified by the NPS results shown in Figure 6. The DPC-CT image reconstructed using the Hilbert filter ($\alpha = 0$) has an excess of its noise power at low spatial frequencies. The reweighted method introduced a certain amount of high frequency power to the final images and shifted the distribution of noises to higher frequencies. This shift increases with larger α.

Edge enhancement provided by the reweighted reconstruction method is quantified by the pseudo-PSF measurement (Figure 7). The width of the PSF decreases with increasing α (i.e., by more than 30% at the 10% PSF), indicating mitigated spatial blurring and improved image sharpness.

4. CONCLUSIONS

In this paper, a new reconstruction method has been proposed to improve the noise properties and object detectabilities in DPC-CT. A processed DPC-CT image is the weighted-sum of two images processed using

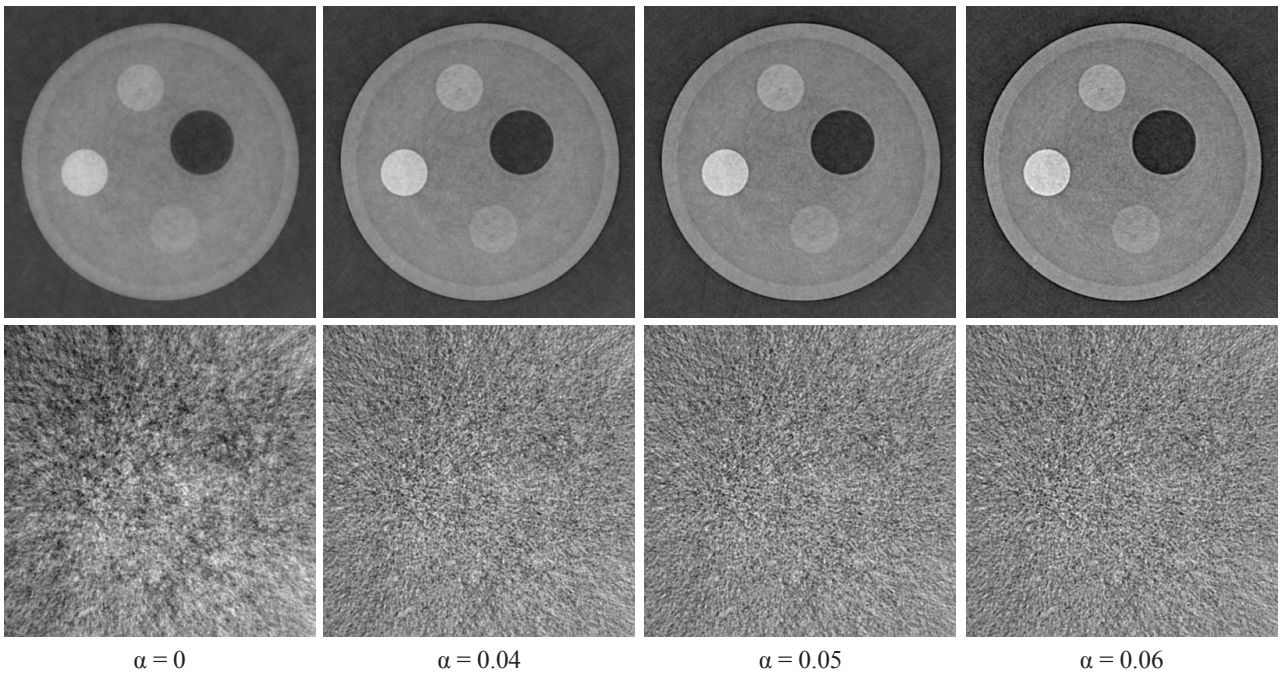

Figure 4. Reweighted DPC-CT images (top row) and corresponding noise-only images (bottom row). $\alpha = 0$ corresponds to DPC-CT reconstruction using a Hilbert filter alone. The DPC-CT images are displayed over [-δ_{H_2O}, 3δ_{H_2O}]. $k_0 = 7$ was used for the tanh filter.

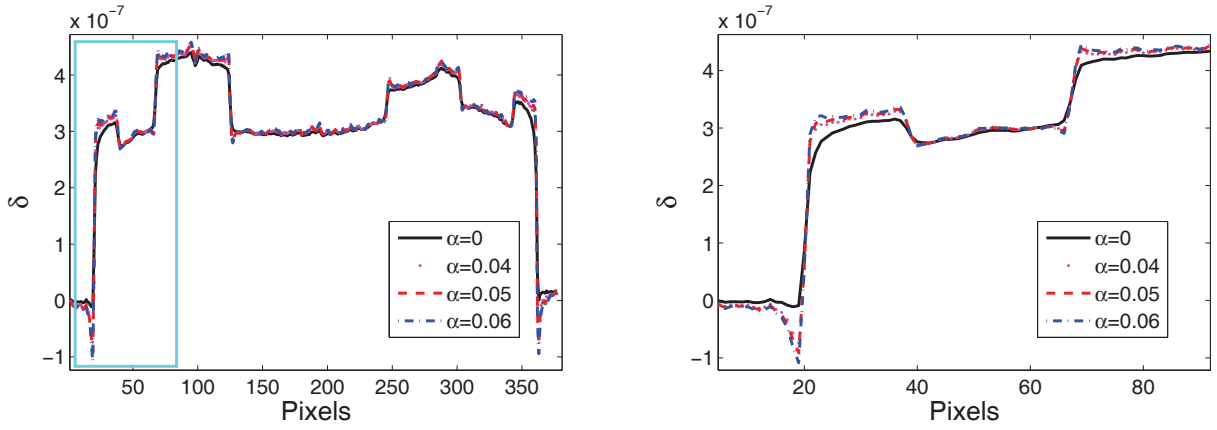

(a) (b)

Figure 5. (a) Comparison of line profiles through DPC-CT images with varying values of reconstruction parameter α along the dashed line in Figure 3. (b) Enlarged rendering of the region indicated by the rectangular box in (a).

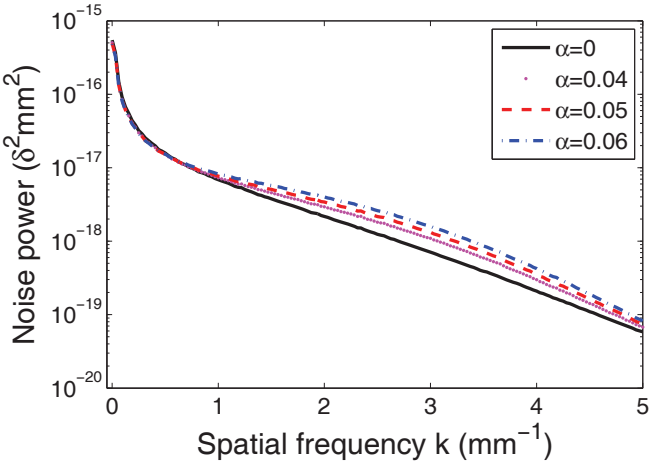

Figure 6. Noise power spectra of reweighted DPC-CT images. The amount of high frequency noise increases with increasing α.

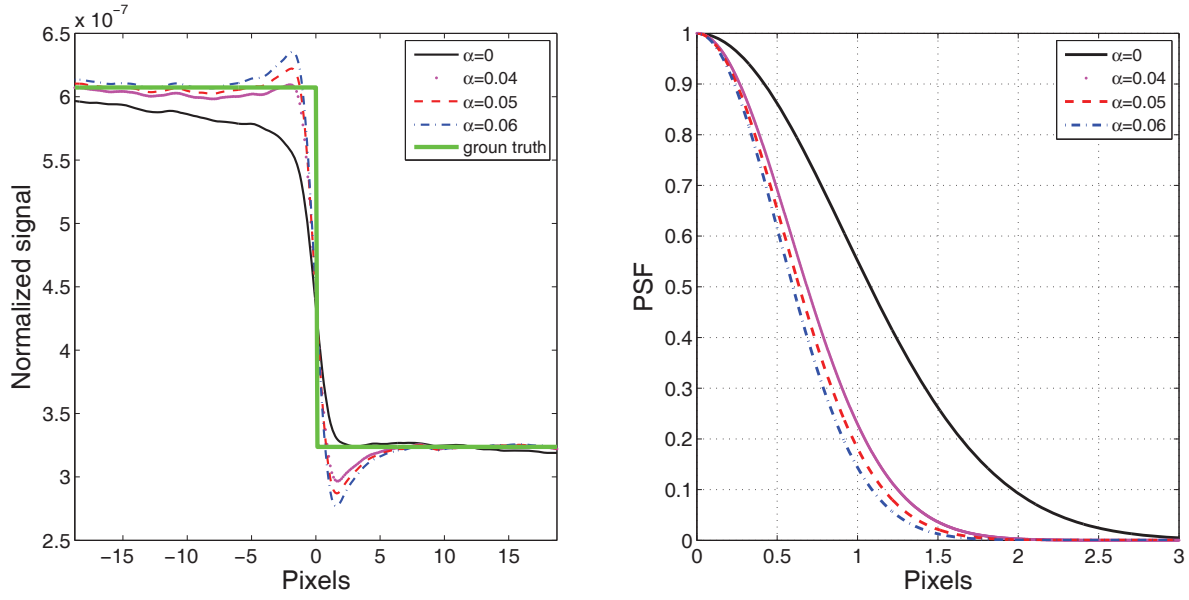

(a) (b)

Figure 7. (a) Radially averaged edge response of the PTFE rod. (b) Point spread function (PSF) corresponds to the measurement in (a).

different techniques. Specifically, the first image is the "original" DPC-CT image reconstructed using the well-established Hilbert filter. For the second image, a hyperbolic tangent filter is used in image reconstruction to regularize the noise power in low spatial frequency regions, which is equivalent to applying a high pass filter to the image. Experimental phantom studies show that DPC-CT images reconstructed using this method have improved visual perception because of enhanced edges and a more "natural" noise texture. NPS measurements show that this method shifts the DPC-CT image's NPS in the high spatial frequency direction and increases the graininess of the image. Image reconstruction accuracy is well maintained by using this method. This method is expected to become a valuable tool to further improve object detectability in DPC-CT.

REFERENCES

1. A. Momose, S. Kawamoto, I. Koyama, Y. Hamaishi, H. Takai, and Y. Suzuki, "Demonstration of x-ray talbot interferometry," *Jpn. J. Appl. Phys., Part 2* **42**(7B), pp. 866–8, 2003.
2. T. Weitkamp, A. Diaz, C. David, F. Pfeiffer, M. Stampanoni, P. Cloetens, and E. Zeigler, "X-ray phase imaging with a grating interferometer," *Opt. Exp.* **12**(16), pp. 6296–304, 2005.
3. F. Pfeiffer, T. Weitkamp, O. Bunk, and C. David, "Phase retrieval and differential phase-contrast imaging with low-brilliance x-ray sources," *Nat. Phys.* **2**, pp. 258–261, Apr 2006.
4. T. Weitkamp, C. David, C. Kottler, O. Bunk, and F. Pfeiffer, "Tomography with grating interferometers at low-brilliance sources," in *Proc. SPIE*, **6318**, p. 63180S, 2006.
5. A. Momose, W. Yashiro, Y. Takeda, Y. Suzuki, and T. Hattori, "Phase tomography by x-ray talbot interferometry for biological imaging," *Japanese Journal of Applied Physics, Part 1 (Regular Papers, Short Notes & Review Papers)* **45**(6A), pp. 5254–62, 2006.
6. J. Zambelli, N. Bevins, Z. Qi, and G.-H. Chen, "Radiation dose efficiency comparison between differential phase contrast CT and conventional absorption CT," *Med. Phys.* **37**, pp. 2473–2479, 2010.

7. G. Chen, J. Zambelli, K. Li, N. Bevins, and Z. Qi, "Scaling law for noise variance and spatial resolution in differential phase contrast computed tomography," *Med. Phys.* **38**, p. 584, 2011.
8. T. Köhler, K. J. Engel, and E. Roessl, "Noise properties of grating-based x-ray phase contrast computed tomography," *Med. Phys.* **38**, p. S106, 2011.
9. R. Raupach and T. Flohr, "Analytical evaluation of the signal and noise propagation in x-ray differential phase-contrast computed tomography," *Phys. Med. Biol.* **56**, p. 2219, 2011.
10. J. Zambelli, K. Li, N. Bevins, Z. Qi, and G. Chen, "Noise characteristics of x-ray differential phase contrast ct," in *Proc. SPIE*, **7961**, p. 79613N, 2011.
11. Z. Qi and G.-H. Chen, "Direct fan-beam reconstruction algorithm via filtered backprojection for differential phase-contrast computed tomography," *X-Ray Opt. Instrum.* **2008**, p. 835172, 2008.
12. J. H. Siewerdsen, I. A. Cunningham, and D. A. Jaffray, "A framework for noise-power spectrum analysis of multidimensional images," *Medical Physics* **29**(11), pp. 2655–2671, 2002.
13. G. Chen, P. Theriault Lauzier, J. Tang, B. Nett, S. lei, J. Zambelli, Z. Qi, N. Bevins, A. Raval, and H. Rowley, "Time-resolved interventional cardiac c-arm cone-beam ct: An application of the piccs algorithm," *Medical Imaging, IEEE Transactions on* **PP**(99), p. 1, 2011.